

TABLE OF CONTENTS

COVER

APPROVAL SHEET

ACKNOWLEDGEMENT i

TABLE OF CONTENTS iv

LIST OF FIGURES vii

LIST OF TABLES xviii

LIST OF APPENDIX xix

ABSTRACT xx

SARI xxii

ABBREVIATION xxiv

CHAPTER 1 – INTRODUCTION 1

1.1 Background 1

1.2 Research Location 5

1.3 Exploration History 6

1.4 Previous Works 7

1.5 Problem Statement 9

1.6 Research Objectives 10

1.7 Dissertation Outline 10

CHAPTER 2 – LITERATURE REVIEW AND BASIC THEORY 12

2.1 Literature Review 12

2.1.1 Regional Geology and Tectonic Setting 12

2.1.1.1 General 12

2.1.1.2 Magmatism 14

2.1.1.3 Tectonic Evolution 17

2.1.2 Physiography 22

2.1.3 Regional Stratigraphy 24

2.1.4 Regional Structures 29

2.1.5 Regional Mineralization 33

2.2 Basic Theory 38

2.2.1 Epithermal Deposits.....	38
2.2.2 High-Sulfidation Epithermal Deposits	41
2.2.2.1 General Characteristics	41
2.2.2.2 Hydrothermal Alteration.....	42
2.2.2.3 Mineralization	44
2.2.2.4 Nature and Characteristics of Hydrothermal Fluids	45
2.2.2.5 Metal Transport and Ore Deposition	46
2.2.2.6 Evolution of HS Epithermal Deposits.....	47
2.3 Hypothesis	50
CHAPTER 3 – RESEARCH METHODOLOGY	52
3.1 Introduction	52
3.2 Research Phases	52
3.2.1 Research Preparation	52
3.2.2 Field Investigation	54
3.2.3 Laboratory Analyses.....	55
3.2.3.1 Mineralogical Study.....	55
3.2.3.2 Mineral Chemistry	59
3.2.3.3 Bulk Rock Geochemistry	60
3.2.3.4 Fluid Inclusion Microthermometry.....	60
3.2.4 Result Data Interpretation.....	62
3.2.5 Reporting	62
CHAPTER 4 – LOCAL GEOLOGY	63
4.1 General	63
4.2 Geology of Cijulang Prospect	63
4.2.1 Lithostratigraphic Units.....	65
4.2.2 Lithogeochemistry	74
4.2.2.1 Major and Trace Element Geochemistry	74
4.2.2.2 REE Geochemistry of Host Rocks.....	78
4.2.3 Geological Structures.....	82
4.3 Discussion	85
CHAPTER 5 – ALTERATION AND MINERALIZATION.....	87

5.1 Introduction	87
5.2 Hydrothermal Alteration	88
5.3 Geochemistry of Altered Rocks	106
5.3.1 REE Behaviors in Hydrothermal Alteration Facies.....	106
5.3.2 Immobile Element Geochemistry and Mass Changes	111
5.3.2.1 Mass Balance Isocon	112
5.3.2.2 Alteration Indices	118
5.4 Mineralization	121
5.4.1 Ore and Gangue Mineralogy	123
5.4.2 Paragenesis of Mineralization.....	130
5.4.3 Geochemistry of Ores	132
5.4.4 Alunite Mineral Chemistry	134
5.5 Discussion	138
CHAPTER 6 – ORIGIN AND CHARACTERISTICS OF HYDRO- THERMAL FLUIDS	142
6.1 Fluid Inclusion Microthermometry	142
6.2 Cijulang Prospect	143
6.2.1 Fluid Inclusion Petrography	143
6.2.2 Microthermometric Data	144
6.2.3 Interpretation	145
6.3 Discussion	149
CHAPTER 7 – SUMMARY AND CONCLUSION	151
7.1 Discussion	151
7.1.1 Cijulang Key Deposit Characteristics.....	151
7.1.2 Alteration Fluids and Mineral Stabilities	152
7.1.3 Ore Fluids and Sulfides Mineral Stabilities.....	156
7.1.4 Genetic Model for the Development of HS system in Cijulang area	159
7.2 Conclusion	164
7.2.1 Recommendation	166
REFERENCES	168

LIST OF FIGURES

Figure		Page
Figure 1.1	Fig. 1.1 Map showing the distribution of magmatic arcs and related mineral deposits in Indonesia (Carlile and Mitchell, 1994).	3
Figure 1.2	Map of West Java showing the location of the research area (Cijulang Prospect), Talegong District, Garut Regency, West Java, Indonesia.....	6
Figure 2.1	2.1 Geography of Indonesia and surrounding regions showing present-day tectonic boundaries and volcanic activity (Hall, 2009).....	13
Figure 2.2	(a) Age of sea-floor basement in Indian Ocean (Johnson et. al, 1976, Bronto, 1989) (b) Cretaceous volcanism in Western Indonesia (Hutchison, 1973; Katili, 1973b, 1975; Sano et al, 1978, Bronto, 1989) (c) Miocene volcanism in Western Indonesia (Katili, 1975) (d) Late Cenozoic to Present volcanism in Western Indonesia (Katili, 1975).....	19
Figure 2.3	Tectonic Map of the West Java area showing the research area (modified after Martodjojo, 1984, 2003).....	21
Figure 2.4	Physiographic sketch map of the West Java area showing the research area (Van Bemmelen, 1949).....	22
Figure 2.5	SRTM image showing the geomorphology of the study area ...	23
Figure 2.6	Sedimentary provinces in West Java Area, Indonesia (Martodjojo, 1984).....	24
Figure 2.7	Table illustrating stratigraphic history of the Bogor Basin, West Java (Martodjojo, 1984).....	25
Figure 2.8	Regional geological map showing the research area (Cijulang Sualan prospect), Papandayan District, Garut Regency, West	

	Java (after Alzwar <i>et al.</i> , 1992)	28
Figure 2.9	Stratigraphic succession of the Papandayan District, Garut Regency, West Java, Indonesia (modified after Verdiansyah <i>et al.</i> , 2012).....	29
Figure 2.10	Structural map of West Java based on surface geological mapping (GRDC maps), and Bouguer gravity anomaly map (Source: Yulianto <i>et al.</i> , 2007).....	30
Figure 2.11	Geological setting and characteristics of low- and high-sulfidation epithermal deposits. (Hedenquist <i>et al.</i> , 2000).....	39
Figure 2.12	Cross-section of alteration zones, characteristics of high-sulfidation deposits, as observed at the Summitville Au-Cu deposit, Colorado (Source: Arribas, 1995).....	43
Figure 2.13	Two stages in evolution of porphyry and epithermal ore deposits (Heinrich <i>et al.</i> , 2004).....	47
Figure 2.14	Model showing the two main stages of evolution of HS deposits (Arribas, 1995).....	49
Figure 3.1	Flow chart illustrating research methods and stages.....	53
Figure 4.1	Geological map of the Cijulang prospect area, Papandayan District, Garut agency, West Java and cross section along X-Y is also shown (modified from PT Antam unpublished map).....	64
Figure 4.2	An exposure of andesite lava (a) at Cisuren stream section and (b) at the confluence of Cilukut stream and Cikhuripan River..	65
Figure 4.3	(a) Andesite lava showing flow nature and (b) propylitically altered andesite lava at Cikahuripan river in the southern part of the Cijulang area.....	66
Figure 4.4	Photomicrograph of andesite lava showing (a) phenocrysts of zoned and twin plagioclase and pyroxene (augite) and (b) trachytic texture in which microlaths of plagioclase are in sub-parallel orientation.....	67
Figure 4.5	Photomicrograph of andesite lava showing (a) two euhedral	

	augite phenocrysts and (b) prominent marginal zoning in pyroxene (augite).	67
Figure 4.6	Argillically altered tuff unit exposed (a) at the confluence of Cisuren stream and Cikahuripan streams and (b) along the section of Cikahuripan river in the southern part of the Cijulang area.	69
Figure 4.7	(a) An outcrop of leached tuff at Cisuru hill and (b) silicified rock (probably tuff) with clear quartz eyes. Patch of vuggy silica is present in the massive silica and show rusty stain due to the oxidation of iron sulfide.	69
Figure 4.8	(a) Photomicrograph of lapilli tuff and (b) silicified crystal-dominated tuff. Quartz fragment show resorbed texture.	70
Figure 4.9	Photomicrograph of (a) lapilli tuff showing large lithic fragment which is smectite-sericite altered and spherulite is seen at the upper right corner and (b) welded tuff containing a glass shard and elongated lapilli.	70
Figure 4.10	(a) An outcrop of andesite unit at Cibuni stream section and (b) mafic xenolith within the andesite unit.	72
Figure 4.11	a) An outcrop of andesite breccia cross cut by quartz veinlet and (b) an exposure of andesite breccia along the Cibuni stream section.	72
Figure 4.12	Photomicrograph of andesite (a) dominated by plagioclase phenocrysts (b) showing the porphyro-aphanitic texture.	73
Figure 4.13	(a) An outcrop of propylitically altered polymict breccias unit exposing along the down stream of Citando stream and (b) an exposure of advanced argillically altered polymict breccias at confluence of Citando stream and Cikahuripan river.	73
Figure 4.14	(a) and (b) Photomicrographs of pyrophyllite-dickite/kaolinite altered breccia unit.	74
Figure 4.15	TAS (total alkalis versus silica) classification diagram for	

	volcanic rocks of Cijulang prospect (After Le Maitre, 2002)....	76
Figure 4.16	Nb/Y vs Zr/Ti plot of volcanic rocks from Cijulang prospect (after Winchester and Floyd, 1977).....	76
Figure 4.17	(a) AFM classification diagram (Irvine and Baragar, 1971). (b) K ₂ O vs SiO ₂ variation diagram. (c) Ti-Zr-Sr diagram (After Pearce and Cann, 1973) and Zr-Ti discrimination diagram (log scale) for volcanic rocks (after Pearce and Cann, 1973) of Cijulang Prospect.....	77
Figure 4.18	Harker variation diagrams for major and trace elements of the volcanic rocks from the Cijulang prospect.....	79
Figure 4.19	Chondrite-normalized spider diagrams for least altered volcanics from Cijulang prospect. Using the normalization and ordering scheme of Nakamura (1974).....	80
Figure 4.20	Trace element concentrations of selected volcanic rocks from Cijulang prospects normalized chondrite meteorites (Thompson, 1982) and plotted from the left to the right in order of increasing compatibility in a small fraction of melt of the mantle and typical spidergram patterns for mid-oceanic ridge (MORB), oceanic island (OIB) and island-arc calc-alkaline basalts normalized according to Thompson et al. (1984).....	81
Figure 4.21	MORB-normalized spider diagrams for selected volcanics from Cijulang prospect. MORB-normalized trace element variation diagram for typical island-arc, Island arc calc-alkaline basalt, and oceanic-island basalts are shown and the order of the elements and values of the normalizing constants are from Pearce (1983).....	82
Figure 4.22	Cikahuripan Fault running in the northern part of the Cijulang prospect and (b) narrow and deep incited Cijulang River valley which runs along the Cikahuripan fault.....	83

Figure 4.23	(a) Slicken side occurs at the eastern side of the Cibuni stream along the Cibuni fault and (b) occurrence of waterfall at the upstream of the Cibuni stream.....	84
Figure 4.24	(a) An exposure of fault breccia and (b) localized ore bodies outcropping at the junction of Cikahuripan Fault and Cijeunjing Fault.....	84
Figure 4.25	Minor folding in the southern part of the study area (a) plunging anticlinal fold and (b) vertical beds of argillically-altered tuff in the northern limb of the anticlinal fold.....	85
Figure 5.1	(a) An outcrop of leached lapill tuff showing the vuggy texture at the Cisuru Hill and (b) massive silica exposing at the peak of Cisuru Hill.....	90
Figure 5.2	(a) Patches of vuggy silica within the masive silica and (b) amorphous silica occurring along the fractures at Cisuru Hill, Cijulang prospect.....	90
Figure 5.3	Silica alteration (a) secondary fine-grained crystalline hydrothermal quartz filling in the groundmass and in the vugs (open nicol) and (b) resorbed primary quartz enclosed within the silicified groundmass of secondary quartz (cross nicol).....	91
Figure 5.4	Quartz-pyrophyllite-dickite/kaolinite altered breccia outcrops (a) in the central part of the Cijulang prospect and (b) at the confluence of Ciseda stream and Cikahuripan River	92
Figure 5.5	(a) Pervasive quartz-kaolinite alteration occurring in lapilli tuff at Cisuru Hill and (b) kaolinite filling in the vug of silica alteration at Limus Hill.....	93
Figure 5.6	(a) Quartz-alunite alteration of drill core sample (DCjl-04.261) (b) kaolinite filling in the vug of massive sulfide (tennantite-chalcopryrite-pyrite) ore (DCjl-04.282.8).....	93
Figure 5.7	Pervasive quartz-kaolinite/dickite-pyrophyllite alteration in hydrothermal breccia (a) open nicol and (b) cross nicol.....	94

Figure 5.8	(a) Quartz-kaolinite-dickite-pyrophyllite altered hydrothermal breccia (cross nicol) and (b) euhedral large diaspore in the advance argillic altered rock (cross nicol).....	94
Figure 5.9	Photomicrographs of diaspore in the advanced-argillic altered hydrothermal breccia (a) (open nicol) and (b) cross nicol.....	94
Figure 5.10	X-ray diffractograms of quartz-kaolinite-pyrophyllite and quartz-alunite pyrite assemblages from AA zone.....	95
Figure 5.11	X-ray diffractograms of quartz-dickite/kaolinite-pyrophyllite and quartz-kaolinite assemblages from AA zone.....	96
Figure 5.12	Reflectance spectra of advanced argillic alteration mineral mixtures from Cijulang prospect from Cijulang prospect.....	97
Figure 5.13	Quartz-kaolinite-illite (argillic) alteration exposing (a) at the southern part of the Cikahuripan River and (b) along the Cibuni stream.....	98
Figure 5.14	Pervasive argillic alteration comprising (a) illite-smectite assemblage (cross nicol) and (b) chlorite-illite assemblages (cross nicol).....	98
Figure 5.15	X-ray diffractograms of argillic mineral assemblage (quartz-illite-kaolinite-smectite).....	99
Figure 5.16	X-ray diffractograms of quartz-illite-chlorite and quartz-illite-smectite-chlorite assemblages from argillic zone.....	100
Figure 5.17	Reflectance spectra of argillic alteration and propylitic mineral mixtures from Cijulang prospect.....	100
Figure 5.18	Chlorite-smectite-epidote alteration in the lapilli tuff unit exposed at the confluence of Cisuren stream and Cikahuripan River and (b) chlorite-epidote-magnetite alteration bearing quartz vein at Cikahuripan River in the middle part of the Cijulang area.....	101
Figure 5.19	Replacement of illite, chlorite, epidote and magnetite in mafic minerals and groundmass of host rock andesite (a) (open nicol)	

	and (b) cross nicol.....	102
Figure 5.20	Sericite, calcite and carbonate replacement in plagioclase phenocrysts and groundmass (a) open nicol and (b) cross nicol.	102
Figure 5.21	Chlorite-smectite replacement in phenocryst and groundmass (a) open nicol) (b) cross nicol.....	102
Figure 5.22	X-ray diffractograms of quartz-chlorite-illite-epidote-calcite assemblage from propylitic alteration zone.....	103
Figure 5.23	X-ray diffractograms of quartz-smectite-illite-chlorite assemblage from propylitic alteration zone.....	104
Figure 5.24	Hydrothermal alteration map of the Cijulang Prospect, Talegong District, Garut Regency, West Java. Cross section along X-Y is also shown (modified after Verdiansyah, 2012)...	105
Figure 5.25	(a) Chondrite-normalized REE patterns of samples from silicic alteration facies rocks (b) advanced argillic (c) propylitic and argillic altered rock facies compared to the unaltered equivalent volcanic rocks.....	109
Figure 5.26	Variations in $(La/Sm)_{cn}$, $(La/Yb)_{cn}$, $(Tb/Yb)_{cn}$ ratios displaying REE fractionation in the hydrothermal altered rock compared to unaltered equivalent original rocks. The $(Eu/Eu^*)_{cn}$ ration shows the variation of Eu anomaly.....	110
Figure 5.27	Isocon plots of un-altered rocks (N=2) and propylitically altered rocks (N=2).....	113
Figure 5.28	Concentration change (ΔC) of un-altered rocks (N=2) and propylitically altered rocks (N=2).	114
Figure 5.29	Isocon plots of un-altered volcanics (N=2) and argillic altered rocks (N=3).....	115
Figure 5.30	Concentration change (ΔC) of un-altered rocks (N=2) and argillic altered rocks (N=2).....	115
Figure 5.31	Isocon plots of argillic altered rocks (N=2) and advance argillic altered rocks (N=3).....	116

Figure 5.32	Concentration change (ΔC) of un-altered volcanic rocks (N=2) and advance argillic altered rocks (N=3).....	116
Figure 5.33	Isocon plots of un-altered volcanic rocks (N=2) and silica alteration (N=2).....	117
Figure 5.34	Concentration change (ΔC) of un-altered volcanic rocks (N=2) and silica alteration (N=2).....	118
Figure 5.35	AI-CCPI box plot of Cijulang altered rocks.....	120
Figure 5.36	AI-HSAI alteration box plot for altered rocks of Cijulang area. Interpreted alteration trends applicable to HS system are also shown on the diagram.....	121
Figure 5.37	(a) Enargite and pyrite mineralization within the vugs of the massive silica at Limus Hill and (b) sulfide (pyrite-enargite) veinlets within the advanced argillically altered hydrothermal breccias.....	122
Figure 5.38	(a) An outcrop of massive silicified ore bodies and (b) Massive ore bodies in the advanced argillic-altered hydrothermal breccias occurring along the Cikahuripan River in the central part of Cijulang area.....	123
Figure 5.39	Fine-grain aggregate of anhedral pyrite replacement within the advanced argillically altered rock (open nicol) (b) pyrite as fracture.....	124
Figure 5.40	(a) Euhedral pyrite grains within networks of alunite laths and native sulfur from the quart-alunite zone (open nicol) and (b) vug-filling anhedral pyrite replaced by enargite and covellite (open nicol).....	125
Figure 5.41	Crackled and eruptive pyrite along the fracture (open nicol) and (b) anhedral pyrite showing zonation within the vug of the silica zone (open nicol).....	125
Figure 5.42	Two large euhedral long prismatic enargite within the vugs of silica alteration in (a) open nicol and (b) cross nicol.....	126

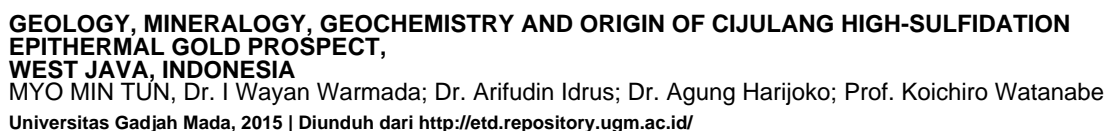
Figure 5.43	Late enargite-luzonite-chalcopyrite vein along the microfracture of silicified rock and (cross nicol) (b) anhedral luzonite intergrown with enargite within the vug of the silica-altered zone (cross nicol).....	127
Figure 5.44	(a) Infill and replacement of injected tennantite within the brecciated pyrite (open nicol) and (b) tennantite containing small bleb of chalcopyrite inclusions along the microfracture (open nicol).....	127
Figure 5.45	Covellite replacement in the enargite within the vug of the silica alteration (a) as disseminated grain (cross nicol) (b) as massive replacement in the enargite mineral (cross nicol).....	128
Figure 5.46	(a) Galena forming as matrix along the fractures associated with enargite, chalcopyrite (open nicol) and (b) galena with enargite ore bornite and pyrite (open nicol).....	129
Figure 5.47	Intergrowth of enargite, luzonite, emplectite and chalcopyrite replacing the pyrite with the vug of the silica (open nicol) and (b) small specs of chalcopyrite inclusion within the large anhedral tennantite which fill the along the fracture (open nicol).....	129
Figure 5.48	(a) Anhedral emplectite in massive tennantite (open nicol) and (b) irregular emplectite associated with intergrowth of enargite, luzonite and chalcopyrite (cross nicol).....	129
Figure 5.49	(a) Minute anhedral telluride within the chalcopyrite grain associated with tennantite and pyrite (open nicol) and (b) small spec of telluride in the chalcopyrite which is intergrown with tennantite (open nicol).....	130
Figure 5.50	Paragenetic sequences of mineralization for Cijulang prospect. Gold is introduced in stage I pyrite-enargite mineralization and more abundant in the stage II associated with tennantite-chalcopyrite-telluride assemblage.....	132

Figure 5.51	Multi-element plot of silver versus Cu, As, Sb, Sn, Zn and Pb.	134
Figure 5.52	SEI micrograph and spectrum of alunite from drill core sample (a) (Dcjl-04-261) and (b) (Dcjl-04-282.8) of the Cijulang prospect.....	136
Figure 5.53	EPMA elemental mapping of hypogene quartz-alunite alteration from Cijulang prospect: distribution of K, Al, S, Na and Ca, showing the zonal and irregular concentration of K and Na, and homogeneous S and Al.....	137
Figure 5.54	Thermal stability of various hydrothermal minerals that occur in the epithermal environment under acid and neutral-pH condition, and the typical temperature range for deposition of epithermal ore (Reyes, 1990, Hedenquist et al., 1996).....	139
Figure 6.1	Photomicrographs of (a) a bi-phase (L+V) liquid-dominated primary fluid inclusions entrapped in the secondary hydrothermal quartz (b) vapor- and liquid-rich inclusions from the primary igneous quartz phenocryst of the vuggy silica alteration zone from Cijulang prospect.....	145
Figure 6.2	Microthermometric data for primary fluid inclusions in quartz from the Cijulang prospect, West Java: (a) frequency distribution of homogenization temperatures of fluid inclusions and (b) salinity (wt.% NaCl eq.) versus average homogenization temperatures (<i>Th</i>) for fluid inclusions.....	146
Figure 6.3	<i>Th</i> vs Salinity diagram illustrating typical ranges for inclusion from different types of deposits (Wilkinson, 2001) and a plot of fluid inclusions from Cijulang prospect.....	147
Figure 6.4	<i>Th</i> vs salinity diagram of Cijulang fluid inclusion and densities (g/cm ³) of vapor-saturated H ₂ O-NaCl solutions (Wilkinson, 2001).....	148
Figure 6.5	Elevation vs temperature diagram showing the plot of homogenization temperature measured in quartz from Cijulang	

	High-sulfidation epithermal prospect.....	149
Figure 7.1	A: Calculated P-T curves in the Al_2O_3 - SiO_2 - H_2O system based on 1Kb stability relationships and thermodynamic data (Hemley et al., 1980). Calculated temperature dehydration reactions for kaolinite at 1Kb are $273\pm 10^\circ\text{C}$ for kaolinite-pyrophyllite-quartz (quartz-saturated) and $300\pm 10^\circ\text{C}$ for kaolinite-pyrophyllite-diaspore (quartz-under-saturated). B: Calculated P-T curves for the same system at low water pressure based on 1Kb stability relationships and derived thermodynamic data.....	154
Figure 7.2	Mineral stability relationships in the system Al_2O_3 - SiO_2 - H_2O at 1Kb (after Hemley et al., 1980).....	155
Figure 7.3	Mineral stability relationships in the system K_2O - Al_2O_3 - SiO_2 - H_2O - SO_3 experimentally determined at 200° and 300°C . Quartz is present and total pressure is 1Kb.....	156
Figure 7.4	$\text{Log}f\text{O}_2$ vs. pH diagram and (b) $\text{Log}f\text{O}_2$ vs. $\text{Log}f\text{S}_2$ diagram at 250°C (Heald et al., 1987). $\text{Log}f\text{O}_2$ is constrained from $\text{Log}f\text{O}_2$ vs. pH diagram.....	157
Figure 7.5	A $\log f\text{S}_2$ vs. temperature diagram showing mineral sulfidation reactions at 1bar.....	158
Figure 7.6	Schematic cross sections illustrating the evolution of the Cijulang high sulfidation epithermal system. A. Generalized alteration-mineralization zoning pattern for telescoped porphyry Cu deposits (Sillitoe, 2010) and location of Cijulang epithermal system. B Main wall-rock alteration stage of the magmatic hydrothermal system. C. Main ore mineralization stage of the epithermal system. D. present-day location of mineralized ore zones in the Cijulang prospect.....	163

LIST OF TABLES

Table		Page
Table 2.1	Classification schemes applied to epithermal deposits (Simmons <i>et al.</i> , 2005)	40
Table 5.1	Alteration indices of Cijulang altered rocks.	119



LIST OF APPENDIX

		Page
Appendix A	Samples location map of Cijulang prospect area, Garut Regency, West Java Indonesia.....	183
Appendix B	Location of samples from Cijulang prospect and various analyses applied in this study.....	184
Appendix C	Result of XRF whole Rock chemical analyses of volcanic rocks from Cijulang Prospect, West Java, Indonesia.....	188
Appendix D	Result of ICP-MS whole rock chemical analyses of volcanic rocks from Cijulang Prospect, West Java, Indonesia.....	191
Appendix E	Alteration mineral assemblages from altered rocks of Cijulang Prospect identified from XRD analysis.....	197
Appendix F	Alteration minerals from Cijulang and Sualan Prospects identified from SWIR spectroscopy.....	199
Appendix G	Fluid inclusion microthermometric data of quartz from Cijulang Prospect, Garut Regency, West Java, Indonesia	200